

Noninterferometric phase retrieval using a fractional Fourier system

Unnikrishnan Gopinathan,¹ Guohai Situ,¹ Thomas J. Naughton,² and John T. Sheridan^{1,*}

¹*School of Electrical, Electronic and Mechanical Engineering, College of Engineering, Mathematical and Physical Sciences, University College Dublin, Belfield, Dublin 4, Ireland*

²*Department of Computer Science, National University of Ireland, Maynooth, County Kildare, Ireland, and University of Oulu, RFMedia Laboratory, Oulu Southern Institute, Vierimaantie 5, 84100 Ylivieska, Finland*

*Corresponding author: john.sheridan@ucd.ie

Received June 8, 2007; accepted October 23, 2007;

posted November 8, 2007 (Doc. ID 83902); published December 14, 2007

The signal extraction method based on intensity measurements in two close fractional Fourier domains is examined by using the phase space formalism. The fractional order separation has a lower bound and an upper bound that depend on the signal at hand and the noise in the optical system used for measurement. On the basis of a theoretical analysis, it is shown that for a given optical system a judicious choice of fractional order separation requires some *a priori* knowledge of the signal bandwidth. We also present some experimental results in support of the analysis. © 2007 Optical Society of America

OCIS codes: 070.2575, 100.5070, 120.5050.

1. INTRODUCTION

Noninterferometric deterministic phase retrieval methods have received considerable attention since the work by Teague [1,2] and Streibl [3]. These methods have been used for a broad range of applications from microscopy [4,5] to astronomy [6], with both fully [7,8] and partially coherent sources [9,10] and wavelengths ranging from the visible to x rays [11]. In a broad sense, all of these methods extract the phase and thereby the complete signal information from single or multiple intensity measurements by using a deterministic algorithm based on the underlying physical model. Most of the deterministic phase retrieval methods are based on the transport of intensity model including the methods of Teague and Streibl.

Another class of methods reconstructs the signal by sampling phase space distribution functions like the ambiguity function (AF) [12–15]. The underlying philosophy of these approaches, generically referred to as *phase space tomography*, is that the phase space distribution functions such as the AF contain the entire signal information. Some methods reconstruct the signal by sampling the entire phase space distribution function in a grid. Semichaevsky and Testorf [16] and Nugent [11] have presented a description of the various deterministic phase retrieval techniques using phase space distribution functions.

Methods have been proposed to extract signal information from the intensity of the fractional Fourier transform (FRT) of the signal. Alieva and co-workers [17–19] proposed a method to reconstruct the signal from two close fractional Fourier power spectra. In the context of metrology, intensity measurements in FRT domains have been used to extract information regarding object tilt and translation [20–22]. Lohmann *et al.* [23] have pointed out that for lossless transmission of information the system

space–bandwidth product should encompass the signal space–bandwidth product, with both signal and system space–bandwidth products being represented as an area in the Wigner domain. Depending on the signal at hand and detector used, FRT systems will provide different quality results as compared with Fresnel transform systems based on free-space propagation as we move from one domain to another [24].

In this paper, we use the phase space formalism to examine the signal recovery methods where the signal is captured in two FRT domains in which the orders of the two optical implementations of the FRT differ by very little. In this case we can describe the two resulting FRT domains, into which the Wigner distribution function (WDF) of the signal has been projected, as being close, since their angular separation in phase space is small. Such a treatment helps us in comparing these methods with the phase space tomographic methods that are based on sampling the entire phase space [12–15]. From the literature it appears that the signal extraction methods based on output intensity measurements at two close FRT domains lead to a lesser number of necessary samples. However, we show that the choice of the necessary fractional order separation needs some *a priori* knowledge of the input signal bandwidth and noise in the optical system. This is because (i) the bandwidth of the signal results in an upper bound on the fractional order separation and, (ii) more important, in a differential method the effect of noise in the system is deleterious and leads to a lower bound on the fractional order separation. Using the example of a quadratic phase signal (which can easily be generated experimentally by using a thin lens), it is shown that for a given noise level in the system a signal with a lower rate of change of spatial frequency has a higher upper bound and can be estimated by using a larger difference in FRT order.

We use an optical system that performs a scale-invariant FRT to experimentally estimate the spatial frequency distribution (local spatial frequency [25]) of input quadratic phase signals generated by two lenses of focal length 8 mm and 20 cm. We use the same fractional order separation to characterize the spatial frequency distribution of both lenses. It is seen that for the 20 cm focal length lens the spatial frequency distribution estimated is erroneous, as the fractional order separation is inadequate to accommodate the measurement of this signal.

2. PROJECTION SLICES IN PHASE SPACE

Let us consider a one-dimensional signal $f(\cdot)$. Let $f_\alpha(\cdot)$ represent the FRT of $f(\cdot)$, defined as

$$f_\alpha(x) = \int f(x_0)K_\alpha(x, x_0)dx_0, \quad (1)$$

where

$$K_\alpha(x, x_0) = \frac{\exp(i\alpha/2)}{\sqrt{i \sin \alpha}} \exp\left[i\pi\left(\frac{x^2}{\tan \alpha} - \frac{2xx_0}{\sin \alpha} + \frac{x_0^2}{\tan \alpha}\right)\right]. \quad (2)$$

The integrals, unless otherwise specified, run from $-\infty$ to $+\infty$. When $\alpha=0$, the kernel $K_\alpha(x, x_0)$ reduces to $\delta(x-x_0)$, and we have $f_0(x)=f(x)$. When $\alpha=\pi$, the kernel $K_\alpha(x, x_0)$ reduces to $\delta(x+x_0)$, and we have $f_\pi(x)=f(-x)$. When $\alpha=\pi/2$ and $\alpha=-\pi/2$, we have the Fourier transform (FT) and inverse FT of the input signal, respectively.

In the following analysis, we use two phase space distributions [25] of the signal—the WDF and the AF. The WDF of $f(\cdot)$, $W(x, \nu)$ is defined as

$$W(x, \nu) = \int f\left(x + \frac{x'}{2}\right)f^*\left(x - \frac{x'}{2}\right)\exp(-i2\pi\nu x')dx', \quad (3)$$

while the AF, $A(\bar{x}, \bar{\nu})$ is

$$A(\bar{x}, \bar{\nu}) = \int f\left(\hat{x} + \frac{\bar{x}}{2}\right)f^*\left(\hat{x} - \frac{\bar{x}}{2}\right)\exp(-i2\pi\bar{\nu}\hat{x})d\hat{x}. \quad (4)$$

The AF is related to the WDF through the FT and inverse FT,

$$A(\bar{x}, \bar{\nu}) = \iint W(x, \nu)\exp[-i2\pi(\bar{\nu}x - \nu\bar{x})]dx d\nu. \quad (5)$$

The zeroth-order moment of the WDF is related to the AF through the FT:

$$A(0, \bar{\nu}) = \int m_0(x)\exp(-i2\pi\bar{\nu}x)dx, \quad (6)$$

where

$$m_0(x) = \int W(x, \nu)d\nu = I_0(x). \quad (7)$$

In Eq. (7), $I_0(x)=|f(x)|^2$ is the intensity of signal $f(x)$. In a similar way the derivative of AF is related to the first-order moment of the WDF:

$$\left.\frac{\partial A(\bar{x}, \bar{\nu})}{\partial \bar{x}}\right|_{\bar{x}=0} = 2\pi i \int m_1(x)\exp(-i2\pi\bar{\nu}x)dx, \quad (8)$$

where

$$m_1(x) = \int \nu W(x, \nu)d\nu = \nu I_0(x). \quad (9)$$

The fractional power spectrum $|f_\alpha(x)|^2$, denoted $I_\alpha(x)$, is equivalent to the radon Wigner transform of the signal-projection of the WDF $W(x, \nu)$ of the signal rotated by an angle α . This equivalence between the radon Wigner transform and the FRT power spectrum was pointed out by Lohmann *et al.* [26] and is written as

$$I_\alpha(x) = \int W(x \cos \alpha - \nu \sin \alpha, x \sin \alpha + \nu \cos \alpha)d\nu. \quad (10)$$

We now proceed to relate the fractional power spectrum, which can be measured by using an optical system performing an FRT, to the AF of the signal. Let $\tilde{I}_\alpha(\bar{\nu})$ denote the FT of $I_\alpha(x)$:

$$\tilde{I}_\alpha(\bar{\nu}) = \int I_\alpha(x)\exp(-i2\pi\bar{\nu}x)dx. \quad (11)$$

Using Eqs. (10) and (11), one can relate $\tilde{I}_\alpha(\bar{\nu})$ to the $A(\bar{x}, \bar{\nu})$ as follows:

$$\tilde{I}_\alpha(\bar{\nu}) = A(\bar{x}, \bar{\nu})|_{\bar{x}=-\bar{\nu} \sin \alpha, \bar{\nu}=\bar{\nu} \cos \alpha}. \quad (12)$$

Taking the FT of the fractional power spectrum of the signal is equivalent to taking a slice through the AF of the signal along $\bar{x}=-\bar{\nu} \sin \alpha$ and $\bar{\nu}=\bar{\nu} \cos \alpha$. To reconstruct the AF, one needs to measure the fractional power spectrum of the signal at all orders. By piecing together the FT of the entire fractional power spectrum at appropriate angles, one can reconstruct the AF and thereby the corresponding signal. Since AF representation has redundancy, it is not necessary to exactly reconstruct the entire AF for signal recovery. Dragoman [27] has shown that the section $\bar{x}=\bar{x}_0$ parallel to the \bar{x} plane contains the entire signal information. However, it is not always possible to access this plane by using optical systems based on linear canonical transforms [24].

For most real-world signals, it may be sufficient to recover the signal by measuring the zeroth- and first-order moments of the WDF as given by Eqs. (6) and (8). Equivalently, one may also use $A(0, \bar{\nu})$ and $\partial A(0, \bar{\nu})/\partial \bar{x}$. In the analysis that follows it may be seen that the latter quantity can be extracted from two intensity measurements in two close FRT domains α_0 and $\alpha_0 + \Delta\alpha$. This is the philosophy underlying the signal recovery approach using two optical implementations of close-fractional-order systems. For the following analysis and without loss of generality we take $\alpha_0=0$. Hence, we can write

$$\tilde{I}_0(\bar{\nu}) = \tilde{I}_{\alpha_0}(\bar{\nu})|_{\alpha_0=0} = A(\bar{x}, \bar{\nu})|_{\bar{x}=0, \bar{\nu}=\bar{\nu}}, \quad (13)$$

$$\tilde{I}_{\Delta\alpha}(\tilde{\nu}) = \tilde{I}_{\alpha_0+\Delta\alpha}(\tilde{\nu})|_{\alpha_0=0} = A(\tilde{x}, \tilde{\nu})|_{\tilde{x}=-\Delta\alpha\tilde{\nu}, \tilde{\nu}=\tilde{\nu}}, \quad (14)$$

where we assume the small-angle approximation $\cos \Delta\alpha \approx 1$ and $\sin \Delta\alpha \approx \Delta\alpha$. Using a first-order Taylor series expansion, we can write that

$$A(\tilde{x} + \Delta\alpha, \tilde{\nu}) \approx A(\tilde{x}, \tilde{\nu}) + \frac{\partial A(\tilde{x}, \tilde{\nu})}{\partial \tilde{x}} \Delta\alpha. \quad (15)$$

Then using Eqs. (15), (13), and (14), we can write

$$\frac{\tilde{I}_{\Delta\alpha}(\tilde{\nu}) - \tilde{I}_0(\tilde{\nu})}{\Delta\alpha} = - \left. \frac{\partial A(\tilde{x}, \tilde{\nu})}{\partial \tilde{x}} \tilde{\nu} \right|_{\tilde{x}=0, \tilde{\nu}=\tilde{\nu}}, \quad (16)$$

and therefore, in the limit $\Delta\alpha \rightarrow 0$,

$$\left. \frac{\partial A(\tilde{x}, \tilde{\nu})}{\partial \tilde{x}} \right|_{\tilde{x}=0} = \int \frac{-1}{\tilde{\nu}} \frac{dI_\alpha(\hat{x})}{d\alpha} \exp(-i2\pi\tilde{\nu}\hat{x}) d\hat{x}. \quad (17)$$

From Eqs. (8) and (9), we know the relation between the local spatial frequency $\nu(x)$ and the first-order derivative of the signal's AF,

$$\nu(x) = \frac{1}{2\pi i} \frac{1}{I_0(x)} \int \left. \frac{\partial A(\tilde{x}, \tilde{\nu})}{\partial \tilde{x}} \right|_{\tilde{x}=0} \exp(i2\pi\tilde{\nu}x) d\tilde{\nu}. \quad (18)$$

Substituting Eq. (17) into Eq. (18) and using the mathematical identity

$$- \frac{1}{\pi i} \int \frac{1}{u} \exp[-i2\pi u(x - \hat{x})] du = \text{sgn}(\hat{x} - x), \quad (19)$$

where sgn denotes the signum function, one obtains an equation [17–19] relating the local spatial frequency $\nu(\cdot)$ to the measured quantity $dI/d\alpha$,

$$\nu(x) = \frac{1}{2I_0(x)} \int \left. \frac{dI_\alpha(\hat{x})}{d\alpha} \right|_{\alpha=0} \text{sgn}(\hat{x} - x) d\hat{x}. \quad (20)$$

In the above discussion, we have assumed the initial FRT order $\alpha_0=0$ for simplicity of analysis. A similar analysis can be done for other values of α_0 in a rotated coordinate system to obtain

$$\nu(x) = \frac{1}{2I_{\alpha_0}(x)} \int \left. \frac{dI_\alpha(\hat{x})}{d\alpha} \right|_{\alpha=\alpha_0} \text{sgn}(\hat{x} - x) d\hat{x}. \quad (21)$$

It may be noted that in the above case the α_0 th FRT of the signal is extracted, from which the signal may be derived by performing an FRT of order $-\alpha_0$. Extending Eq. (20) to two dimensions, it can be shown that

$$\nu_x(x, y) = \frac{\partial \phi(x, y)}{\partial x} = \frac{-1}{2I_{0,0}(x, y)} \iint \left. \frac{\partial I_{\alpha_x, \alpha_y}(\tilde{x}, \tilde{y})}{\partial \alpha_x} \right|_{\alpha_x=0, \alpha_y=0} \times \text{sgn}(x - \tilde{x}) \delta(y - \tilde{y}) d\tilde{x} d\tilde{y} \quad (22)$$

for the case when $\alpha_x \neq \alpha_y$ (anamorphic systems) and

$$\nu_x(x, y) = \frac{\partial \phi(x, y)}{\partial x} = \frac{-1}{2I_0(x, y)} \iint \left. \frac{dI_\alpha(\tilde{x}, \tilde{y})}{d\alpha} \right|_{\alpha=0} \times \text{sgn}(x - \tilde{x}) \delta(y - \tilde{y}) d\tilde{x} d\tilde{y} \quad (23)$$

when $\alpha_x = \alpha_y = \alpha$. Similarly, we can write the equation for the spatial frequency component in the y direction by interchanging the roles of x and y .

The phase $\phi(x, y)$ can then be calculated as

$$\phi(x, y) = \int_k^x \nu_x(x, y) dx + \int_k^y \nu_y(x, y) dy, \quad (24)$$

where k is a constant.

As an example, consider the signal $f(x) = \exp[2\pi i(b_2 x^2 + b_1 x + b_0)]$. The WDF of this signal is $W(x, \nu) = \delta(2b_2 x + b_1 - \nu)$, and using Eq. (10) we can write the fractional power spectrum as

$$I_\alpha(x) = \int \delta(m_1 x - m_2 \nu + b_1) d\nu,$$

where

$$m_1 = 2b_2 \cos \alpha - \sin \alpha, \quad m_2 = 2b_2 \sin \alpha + \cos \alpha. \quad (25)$$

Rescaling the coordinates, we can rewrite this as

$$I_\alpha(x') = \frac{1}{m_2} \int \delta(x' - \nu + b_1) d\nu, \quad x' = m_1 x. \quad (26)$$

In this case,

$$\left. \frac{dI_\alpha(x')}{d\alpha} \right|_{\alpha=0} = -2b_2 \int \delta(x' - \nu + b_1) d\nu, \quad x' = 2b_2 x, \quad (27)$$

and Eq. (20) can therefore be written as

$$\nu(x) = \frac{1}{2I_0(x)} \int \left. \frac{dI_\alpha(x')}{d\alpha} \right|_{\alpha=0} \text{sgn}\left(\frac{x'}{2b_2} - x\right) \frac{dx'}{2b_2}. \quad (28)$$

Assuming uniform intensity in the image plane ($\alpha_0 = 0$), i.e., a pure phase object, $I_0(x) = 1$, and substituting $dI_\alpha/d\alpha$ from Eq. (27) into Eq. (28), after some simplification Eq. (28) reduces to the expected result $\nu(x) = 2b_2 x + b_1$.

3. CHOICE OF FRACTIONAL ORDERS

For practical purposes, how close should the two FRT orders be? To answer this question, we refer to Fig. 1, where a top view of the AF $A(\tilde{x}, \tilde{\nu})$ of a one-dimensional signal, as given by Eq. (4), is presented to illustrate sampling considerations. Shown in the figure are samples (indicated by dots) of two slices of the AF. One slice is along the $\tilde{\nu}$ axis, and the second passes through the origin and is at an angle $\alpha = \Delta\alpha$ to the $\tilde{\nu}$ axis. The samples correspond to the FT of the two intensity measurements at FRT orders $\alpha = 0$ and $\alpha = \Delta\alpha$ [See Eqs. (13) and (14)]. For Eq. (16) to be satisfied for all values of $\tilde{\nu}$,

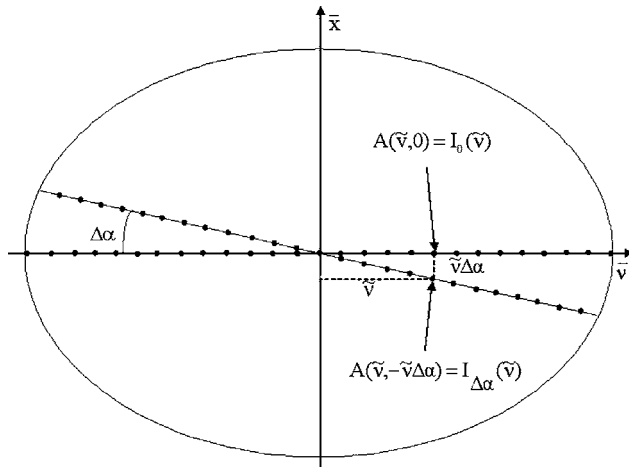


Fig. 1. Schematic representation (top view) of the AF of the one-dimensional signal illustrating sampling considerations. For illustration, the figure is greatly exaggerated and simplified. The dots indicate samples of the FT of the two intensity measurements at FRT orders 0 and $\Delta\alpha$. The two arrows indicate the values $A(\bar{v}, 0)$ and $A(\bar{v}, -\bar{v}\Delta\alpha)$ of the two samples at $(\bar{v}, 0)$ and $(\bar{v}, -\bar{v}\Delta\alpha)$.

$$(\Delta\bar{v}/2)\tan\Delta\alpha < \delta\bar{x}, \quad (29)$$

where $\Delta\bar{v}$ is the full bandwidth of the signal and $\delta\bar{x}$ is the sample separation rate along \bar{x} . The full bandwidth is defined from a Nyquist perspective as the width containing greater than 99% of the total signal power. To satisfy the Nyquist sampling criteria, $\delta\bar{x} \leq 1/\Delta\bar{v}$. This places an upper bound on $\Delta\alpha$ indicating that

$$\Delta\alpha < 2/\Delta\bar{v}^2. \quad (30)$$

The lower bound on $\Delta\alpha$ is dictated by noise in the system. Assuming the noise to be a stationary random process, let N_0 be the power spectral density of the noise in the system. Once again, let $\Delta\bar{v}$ denote the operating bandwidth of the signal. The separation of the fractional orders $\Delta\alpha$ of the two measurements $I_0(x)$ and $I_{\Delta\alpha}(x)$ in Eq. (16) should satisfy the inequality

$$\int_{-\Delta\bar{v}/2}^{\Delta\bar{v}/2} |\tilde{I}_{\Delta\alpha}(\bar{v}) - \tilde{I}_0(\bar{v})|^2 d\bar{v} > N_0\Delta\bar{v}. \quad (31)$$

Equation (31) states that the choice of $\Delta\alpha$ should be such that the energy of the difference signal $[I_{\Delta\alpha} - I_0](\cdot)$ should be greater than the noise power $N_0\Delta\bar{v}$.

Taking the example discussed in the previous section, $f(x) = \exp[2\pi i(b_2x^2 + b_1x + b_0)]$, let us calculate the upper bound and the lower bound on $\Delta\alpha$. If W is the width of the detector array used, then the bandwidth $\Delta\bar{v} = b_2W$. The upper bound on $\Delta\alpha$ may be written as

$$\Delta\alpha < 2/b_2^2W^2. \quad (32)$$

From Eq. (25), we can write the FT of the measured signals $I_0(x)$ and $I_{\Delta\alpha}(x)$ as

$$\tilde{I}_0(\nu) = \exp\left(\frac{i\pi\nu b_1}{b_2}\right)\delta(\nu),$$

$$\tilde{I}_{\Delta\alpha}(\nu) = \frac{1}{2b_2\Delta\alpha + 1} \exp\left(\frac{i2\pi\nu b_1}{2b_2 - \Delta\alpha}\right)\delta(\nu). \quad (33)$$

Substituting from Eq. (33) into Eq. (31) and after some algebraic manipulations we obtain

$$\left[\frac{1}{1 + (2b_2\Delta\alpha)^{-1}}\right]^2 > N_0\Delta\bar{v}. \quad (34)$$

Therefore,

$$\Delta\alpha > \frac{1}{2b_2[(N_0b_2W)^{-1/2} - 1]}. \quad (35)$$

Equation (35) suggests that $N_0 = 0$, i.e., when there is no noise, $\Delta\alpha$ can take arbitrarily low values. As N_0 increases, the lower bound of $\Delta\alpha$ increases. In the above example, the lower bound on $\Delta\alpha$ also depends on the rate of change of frequency b_2 of the chirp signal. From Eq. (34) it may be seen that for a given noise level in the system the signal-to-noise ratio is higher for a signal with a larger value of b_2 . In other words, the effects of noise become more pronounced as the signal frequency becomes lower. Thus, for a given system noise, a fractional order separation that is suitable for a quadratic phase signal with a high value of b_2 may lead to erroneous results for a signal with a low value of b_2 . This prediction is experimentally validated in Section 5. Equations (30) and (31) act so as to limit the range of values $\Delta\alpha$ can assume, which allows accurate measurements to be performed given *a priori* knowledge of the signal bandwidth. Thus the optimal choice of $\Delta\alpha$ requires some *a priori* knowledge of the signal bandwidth and the noise in the system. Though this method requires only $2N$ samples as compared with N^2 samples required for methods that sample the entire phase space [12–15], more *a priori* knowledge of the signal is required, as compared with these latter methods, for the judicious choice of FRT orders α_0 and $\alpha_0 + \Delta\alpha$.

Equation (21) exhibits singularity behavior when $I_{\alpha_0} = 0$. This can be avoided by choosing FRT domains close to orders $\alpha = 0$ or $\alpha = \pi$. As suggested by Teague [2], the sharp irradiance nulls are filled in by defocusing. Also, the choice of α_0 is dictated by practical considerations like walk-off in the system due to apertures.

4. SLICES IN PHASE SPACE USING A SCALE-INVARIANT FRT SYSTEM

The quantity $dI_\alpha(\cdot)/d\alpha$ in Eq. (23) can be measured by using a scale-invariant FRT system [28] comprising two spherical lenses of focal length f separated by a distance d_2 . The input plane and output planes are at distances d_1 from the first and second lenses, respectively. The optical fields in the input and output planes of the optical system are related by a two-dimensional scale-invariant FRT given by

$$f_\alpha(sx, sy) = \iint f(s\tilde{x}, s\tilde{y})K_\alpha(x, y; \tilde{x}, \tilde{y})d\tilde{x}d\tilde{y}, \quad (36)$$

where

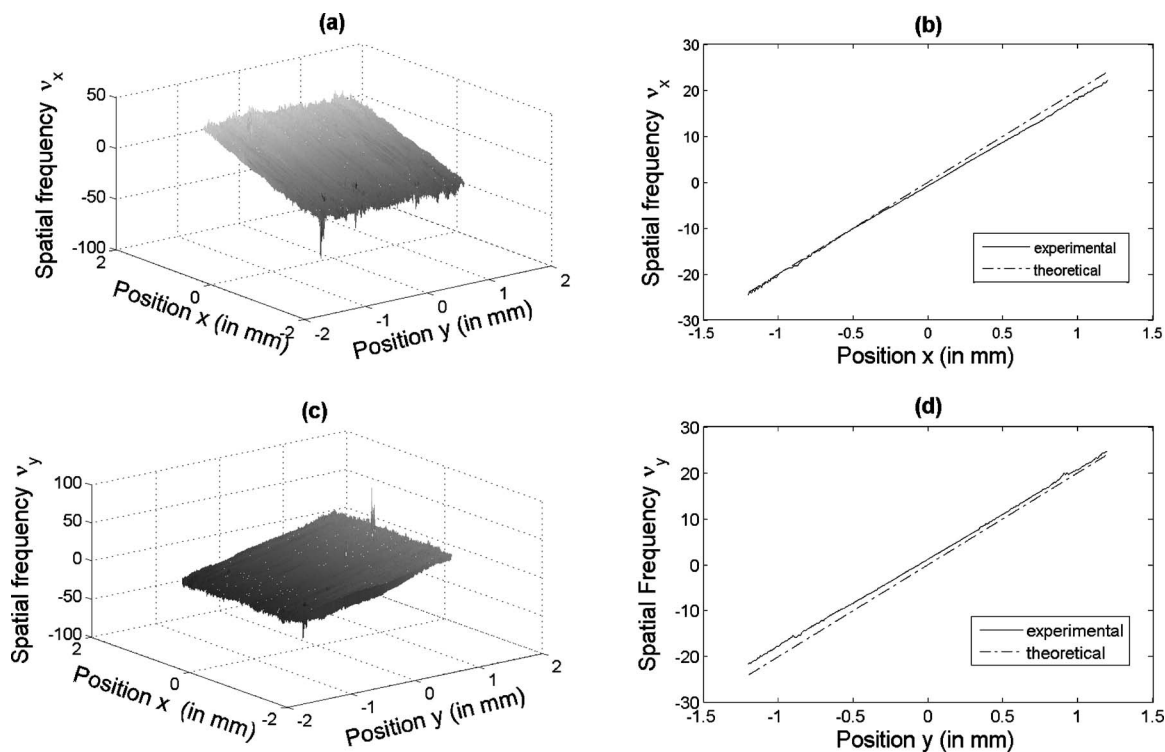


Fig. 2. Experimental results for 8 mm focal length lens (diameter 3 mm): (a) spatial frequency ν_x ; (b) spatial frequency ν_x with the y direction averaged out; (c) spatial frequency ν_y ; (d) spatial frequency ν_y with the x direction averaged out. The dashed-dotted lines in (b) and (d) indicate the predicted spatial frequency corresponding to an 8 mm focal length lens.

$$K_\alpha(x,y;\tilde{x},\tilde{y}) = \exp \left[i\pi \left(\frac{x^2 + y^2}{\tan \alpha} - \frac{2x\tilde{x} + 2y\tilde{y}}{\sin \alpha} + \frac{\tilde{x}^2 + \tilde{y}^2}{\tan \alpha} \right) \right]. \tag{37}$$

(x,y) and (\tilde{x},\tilde{y}) are coordinates in the output and input planes, respectively, α is the FRT order, and s is a scaling

factor. If the distances d_1 and d_2 are related by

$$d_2 = 2f \frac{d_1(d_1 - f) + f^2}{(f - d_1)^2 + f^2}, \tag{38}$$

then the system performs a FRT of order α given by

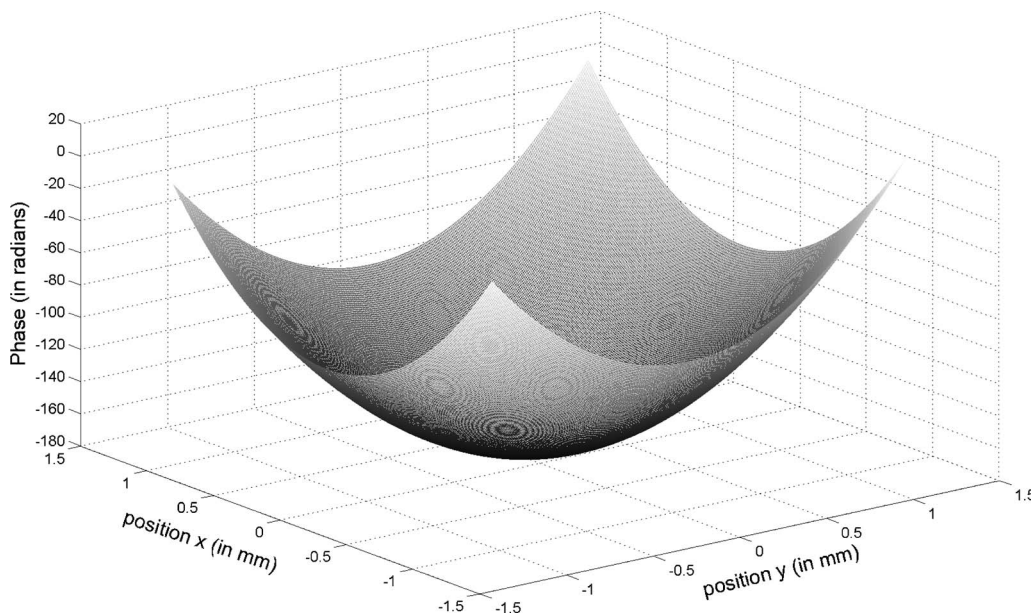


Fig. 3. Phase calculated from the estimated spatial frequency for the 8 mm focal length lens.

$$\alpha = \cos^{-1} \left[\frac{d_1(d_1 - 2f)}{(f - d_1)^2 + f^2} \right]. \quad (39)$$

The scale factor s in Eq. (36) is given by $s = \sqrt{\lambda f}$, where λ is the wavelength of the light. It may be seen that $d_1 = f$ and $d_2 = 2f$ give $\alpha = 2$, corresponding to imaging with a magnification -1 , while setting $d_1 = 0$ and $d_2 = f$ gives $\alpha = 0$, corresponding to imaging with magnification 1.

To estimate the quantity $dI_\alpha(\cdot)/d\alpha$, the FRT system is configured to perform FRT of orders α_1 and α_2 separated by a small value $\Delta\alpha$. The orders are so chosen that $(\alpha_1 + \alpha_2)/2 \approx 0$. The corresponding intensities, I_{α_1} and I_{α_2} , are measured at the output of the optical system. Then the rate of change is approximated by

$$\left. \frac{dI_\alpha(x)}{d\alpha} \right|_{\alpha=0} \approx \frac{I_{\alpha_1}(x) - I_{\alpha_2}(x)}{\Delta\alpha}, \quad (40)$$

$$I_0(x) \approx \frac{I_{\alpha_1}(x) + I_{\alpha_2}(x)}{2}. \quad (41)$$

By measuring I_{α_1} and I_{α_2} , the local spatial frequency components in the x and y directions, $\nu_x(\cdot)$ and $\nu_y(\cdot)$, can be estimated by using Eqs. (22) and (41).

5. EXPERIMENT

We estimated the curvature of the field created by a thin spherical lens [29] of focal length 8 mm and clear aperture 3 mm. The lens was placed in the input plane of an FRT system and illuminated by a collimated laser beam

($\lambda = 633$ nm). For a plane-wave input, under the paraxial approximation the field immediately after the spherical lens is given by $f(x, y) = \exp[j\pi(x^2 + y^2)/\lambda f_i]$, where f_i is the focal length of the lens in the two orthogonal x and y directions. This is the two-dimensional extension of the one-dimensional chirp signal discussed in Sections 2 and 3 with $b_2 = 1/2\lambda f_i$ and $b_1 = 0$. If the lens is tilted with respect to the optical axis of the system, the value of b_1 is non-zero. The optical system performs a scale-invariant optical FRT with the input and output coordinates scaled by a factor $s = \sqrt{\lambda f}$, where f is the focal length of the lens used in the FRT system [see Eq. (36)]. Accounting for this scaling, $b_2 = f/2f_i$, and the spatial frequency as measured by the system is f/f_i .

With the 8 mm lens placed at the input, the optical system is first configured to obtain a FRT order $\alpha = \pi$ ($f = 160$ mm, $d_1 = 160$ mm, and $d_2 = 320$ mm), and the first intensity measurement is performed. This is preferred, for practical reasons, to the $\alpha = 0$ system configuration, where the input and output planes coincide with the plane of the lenses. The second intensity measurement is done by perturbing the fractional order by a small value $\Delta\alpha = 0.006$ corresponding to a perturbation in d_1 by 0.5 mm and d_2 by 1 mm. The intensity measurements were performed with a CCD (Imperx Model, 1024×1024 pixels, $7.6 \mu\text{m}$ square pixel). The width of the sensor array is $W = 8$ mm in both x and y directions. Figure 2(a) shows the value of ν_x estimated by using Eq. (22). Figure 2(b) shows ν_x averaged along the y direction. Plotted as the dashed-dotted line is the theoretically expected curve with the value $b_2 = 20$ and $b_1 = 0$ for $f = 160$ mm and $f_i = 8$ mm. The difference in the experimentally deter-

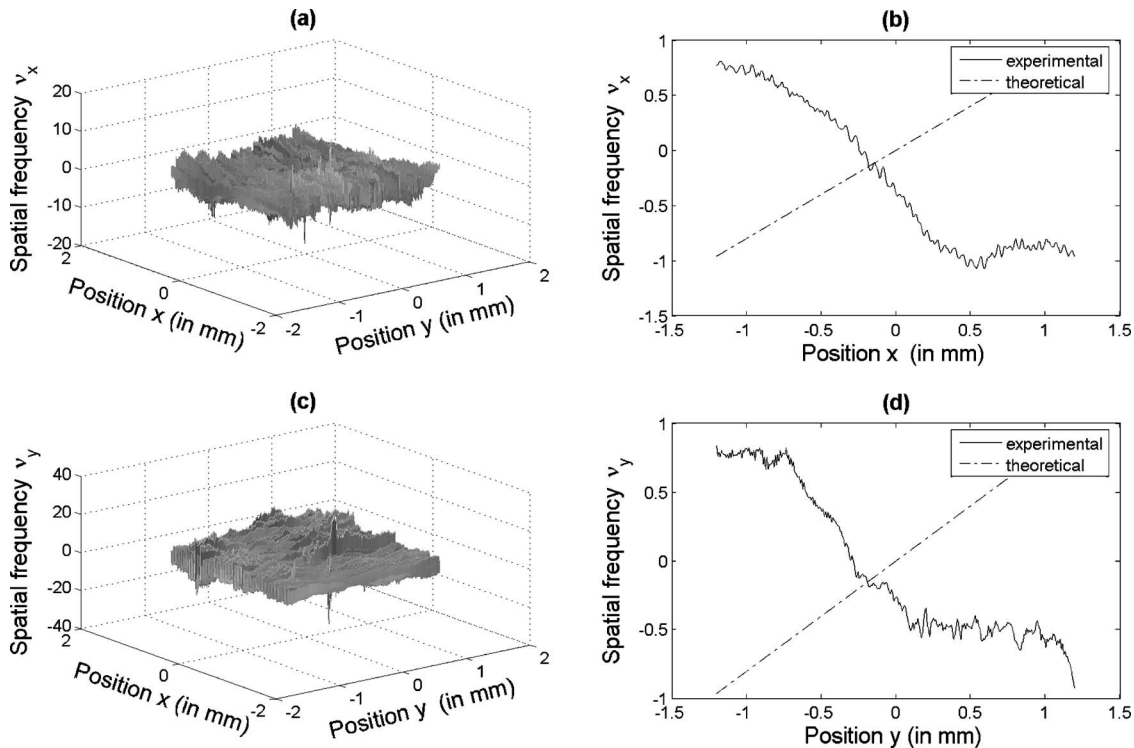


Fig. 4. Experimental results for the 20 cm focal length lens: (a) spatial frequency ν_x ; (b) spatial frequency ν_x with the y direction averaged out; (c) spatial frequency ν_y ; (d) spatial frequency ν_y with the x direction averaged out. The dashed-dotted lines in (b) and (d) indicate the predicted spatial frequency corresponding to a 20 cm focal length lens.

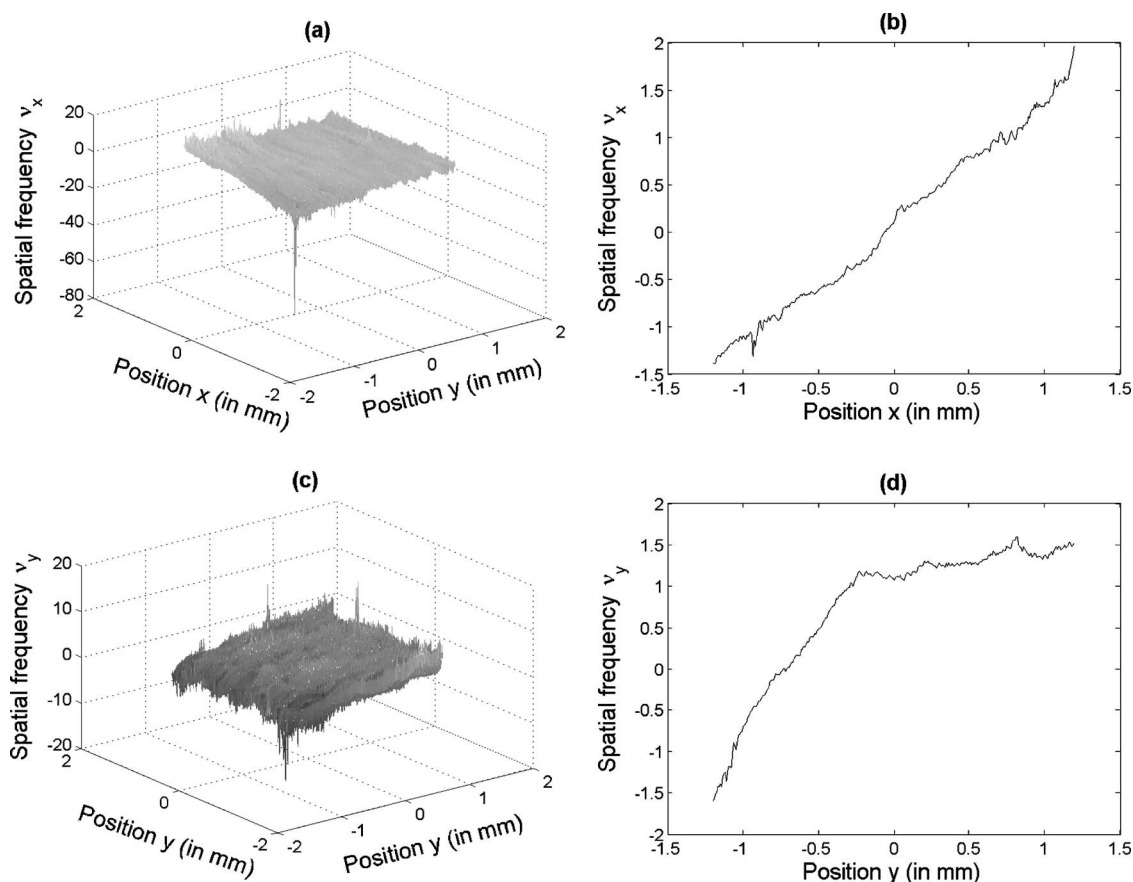


Fig. 5. Collimated beam input: (a) spatial frequency v_x ; (b) spatial frequency v_x with the y direction averaged out; (c) spatial frequency v_y ; (d) spatial frequency v_y with the x direction averaged out.

mined curve and the theoretically expected curve may be attributed to various experimental errors. The main sources of experimental errors are the positioning errors of the lenses leading to errors in the distances d_1 and d_2 , errors in collimation of the beam, and tilt of components with respect to the optical axis of the system. The estimated values of the focal length from the experimentally determined curve were $f_y = 8.36$ mm and $f_x = 8.3$ mm. Figure 3 shows the phase estimated from the spatial frequency shown in Fig. 2.

Figure 4 shows the plots corresponding to a lens of focal length 20 cm. The measurements were carried out for the same FRT order separation, $\Delta\alpha = 0.006$, used in the previous case. As can be seen from the plots, this fractional order separation leads to an erroneous detection of spatial frequency. For this case, the value of $b_2 = 0.8$ leads to a higher value of the lower bound than predicted by Eq. (35).

For completeness, in Fig. 5 we show the results for the case when there is no input signal. The measurements were carried out for the same FRT order separation, $\Delta\alpha = 0.006$, used in the previous case and collimated illumination. The result therefore corresponds to noise and drifts in the system and places a lower threshold on performance.

6. CONCLUSION

In this paper, we examined the signal recovery methods that use two intensity measurements in two close FRT do-

main, using the phase space formalism. Although these methods require fewer samples than phase tomographic methods that sample the entire phase space, the choice of the fractional order separation needs *a priori* knowledge of the signal bandwidth and noise level of the optical system used for measurement. This is because (i) the bandwidth of the signal results in an upper bound on the fractional order separation and, furthermore and very significantly, (ii) the noise in the system leads to a lower bound on the FRT order separation. Using the example of a quadratic phase signal, we have shown that for a given noise level in the system, signals with a lower rate of change of spatial frequency have a higher upper bound.

We used a scale-invariant fractional Fourier optical system to experimentally estimate the spatial frequency distribution of quadratic phase signals generated by two lenses of focal length 8 mm and 20 cm. Using the same fractional order separation for both the lenses, it was found that for the case of the 20 cm focal length lens the spatial frequency estimated is erroneous, as the fractional order separation is inadequate to extract this signal.

ACKNOWLEDGMENTS

We acknowledge the support of Enterprise Ireland and Science Foundation Ireland through the Research Innovation and Proof of Concept Funds, the Basic Research and Research Frontiers Programmes. We thank the Irish

Research Council for Science, Engineering and Technology. We thank a reviewer for his or her comments.

REFERENCES

1. M. R. Teague, "Deterministic phase retrieval: a Green's function solution," *J. Opt. Soc. Am.* **73**, 1434–1441 (1983).
2. M. R. Teague, "Image formation in terms of transport equation," *J. Opt. Soc. Am. A* **2**, 2019–2026 (1985).
3. N. Streibl, "Phase imaging by the transport equation of intensity," *Opt. Commun.* **49**, 6–10 (1984).
4. A. Barty, K. A. Nugent, D. Paganin, and A. Roberts, "Quantitative optical phase microscopy," *Opt. Lett.* **23**, 817–819 (1998).
5. M. Jayashree, G. K. Dutta, and R. M. Vasu, "Optical tomographic microscope for quantitative imaging of phase objects," *Appl. Opt.* **39**, 277–283 (2000).
6. F. Roddier, "Wavefront sensing and the irradiance transport equation," *Appl. Opt.* **29**, 1402–1403 (1990).
7. K. Ichikawa, A. W. Lohmann, and M. Takeda, "Phase retrieval based on irradiance transport equation and the Fourier transport method," *Appl. Opt.* **27**, 3433–3436 (1988).
8. G. K. Datta and R. M. Vasu, "Noninterferometric methods of phase estimation for application in optical tomography," *J. Mod. Opt.* **46**, 1377–1388 (1999).
9. D. Paganin and K. A. Nugent, "Noninterferometric phase imaging with partially coherent light," *Phys. Rev. Lett.* **80**, 2586–2589 (1998).
10. T. E. Gureyev, A. Roberts, and K. A. Nugent, "Partially coherent fields, the transport-of-intensity equation, and the phase uniqueness," *J. Opt. Soc. Am. A* **12**, 1942–1946 (1995).
11. K. A. Nugent, "X-ray noninterferometric phase imaging," *J. Opt. Soc. Am. A* **24**, 536–547 (2007).
12. J. Tu and S. Tomura, "Wave field determination using tomography of the ambiguity function," *Phys. Rev. E* **55**, 1946–1949 (1997).
13. J. Tu and S. Tomura, "Analytical relation for recovering the mutual intensity by means of intensity information," *J. Opt. Soc. Am. A* **15**, 202–206 (1998).
14. D. F. McAlister, M. Beck, L. Clarke, A. Mayer, and M. G. Raymer, "Optical phase retrieval by phase-space tomography and fractional-order Fourier transforms," *Opt. Lett.* **20**, 1181–1183 (1995).
15. M. G. Raymer, M. Beck, and D. F. McAlister, "Complex-wavefield reconstruction using phase-space tomography," *Phys. Rev. Lett.* **72**, 1137–1140 (1994).
16. A. Semichaevsky and M. Testorf, "Phase-space interpretation of deterministic phase retrieval," *J. Opt. Soc. Am. A* **21**, 2173–2179 (2004).
17. T. Alieva and M. J. Bastiaans, "Phase-space distributions in quasi-polar coordinates and the fractional Fourier transform," *J. Opt. Soc. Am. A* **17**, 2324–2329 (2000).
18. T. Alieva and M. J. Bastiaans, "On fractional Fourier moments," *IEEE Signal Process. Lett.* **7**, 320–323 (2000).
19. T. Alieva, M. J. Bastiaans, and L. Stankovic, "Signal reconstruction from two close fractional Fourier power spectra," *IEEE Trans. Signal Process.* **51**, 112–123 (2003).
20. J. T. Sheridan and R. Patten, "Holographic interferometry and the fractional Fourier transformation," *Opt. Lett.* **25**, 448–450 (2000).
21. J. T. Sheridan, B. M. Hennelly, and D. P. Kelly, "Motion detection, the Wigner distribution function, and the optical fractional Fourier transform," *Opt. Lett.* **28**, 884–886 (2003).
22. D. P. Kelly, J. E. Ward, U. Gopinathan, B. M. Hennelly, F. T. O' Neill, and J. T. Sheridan, "Paraxial speckle based metrology system with an aperture," *J. Opt. Soc. Am. A* **23**, 2861–2870 (2006).
23. A. W. Lohmann, R. G. Dorsch, D. Mendlovic, Z. Zalevsky, and C. Ferreira, "Space-bandwidth product of optical signals and systems," *J. Opt. Soc. Am. A* **13**, 470–473 (1996).
24. B. M. Hennelly and J. T. Sheridan, "Generalizing, optimizing, and inventing numerical algorithms for the fractional Fourier, Fresnel, and linear canonical transforms," *J. Opt. Soc. Am. A* **22**, 917–927 (2005).
25. M. J. Bastiaans, "Application of Wigner distribution function in optics," in *Wigner Distribution—Theory and Applications in Signal Processing*, W. Mecklenbraüker and F. Hlawatsch, eds. (Elsevier Science, 1997), pp. 375–426.
26. A. W. Lohmann and B. H. Soffer, "Relationship between the Radon–Wigner and fractional Fourier transforms," *J. Opt. Soc. Am. A* **11**, 1798–1801 (1994).
27. D. Dragoman, "Redundancy of phase-space distribution functions in complex field recovery problems," *Appl. Opt.* **42**, 1932–1937 (2003).
28. L. Z. Cai and Y. Q. Yang, "Optical implementation of scale invariant fractional Fourier transform of continuously variable orders with a two-lens system," *Opt. Laser Technol.* **34**, 249–252 (2002).
29. www.edmundoptics.com, Part No. NT45-045.